Appl Biochem Biotechnol (2009) 159:261–269
DOI 10.1007/s12010-008-8390-1

Direct Observation of Single Molecule Conformational Change of Tight-Turn Paperclip DNA Triplex in Solution

Ching-Ping Liu · Ming-Tsai Wey · Chia-Ching Chang · Lou-Sing Kan

Received: 21 August 2008 / Accepted: 30 September 2008 /
Published online: 18 October 2008

Abstract DNA triplex modulates gene expression by forming stable conformation in physiological condition. However, it is not feasible to observe this unique molecular structure of large molecule with 54 oligodeoxynucleotides directly by conventional nuclear magnetic approach. In this study, we observed directly single molecular images of paperclip DNA triplexes formation in a buffer solution of pH 6.0 by atomic force microscopy (AFM). Meanwhile, a diffuse "tail" of unwound DNA was observed in pH 8.0 solution. This designable approach in visualizing the overall structures and shapes of oligo-DNAs at the single molecular level, by AFM, is applicable to other biopolymers as well.

Keywords DNA triplex · Atomic force microscopy · Tight-turn paperclip DNA · Single molecule image

Abbreviations

AFM	atomic force microscopy
TFOs	triplex-forming oligodeoxynucleotides
NMR	nuclear magnetic resonance
CD	circular dichroism
PITPNM 3	phosphatidylinositol transfer protein membrane-associated genes

C.-P. Liu · M.-T. Wey · L.-S. Kan (✉)
Institute of Chemistry, Academia Sinica, Taipei 11529, Taiwan
e-mail: lskan@chem.sinica.edu.tw

M.-T. Wey
College of Life Science, National Tsinghua University, Hsinchu 300, Taiwan

C.-C. Chang (✉)
Department of Biological Sciences and Technology, National Chiao Tung University, 75 Po-Ai Street, Hsinchu 30050, Taiwan
e-mail: ccchang01@faculty.nctu.edu.tw

C.-C. Chang
Institute of Physics, Academia Sinica, Taipei 11529, Taiwan

L.-S. Kan
Department of Bioengineering, Tatung University, Taipei 104, Taiwan

Introduction

DNA triplex plays important roles in controlling gene expression and modulation. Its formation and structural characterization are of prime interest [1–8]. A thorough investigation of the structural features of triplex DNA is critical to the overall understanding of the biological functions and the possible therapeutic uses of triplex-forming oligodeoxynucleotides (TFOs). Previous study indicated that the Watson–Crick base pairs by natural bases can form a triplex with parallel back-folded adenine strand regions even at pH 7.0 [9]. Meanwhile, the TFO-directed triple helix (triplex) DNA formation revealed that the sequence 5′-TCTCTCCTCTCTAGAGAG-3′ (featuring repeated AG or GA sequences) is capable of forming intramolecular triple helix in slightly acidic solutions by folding into a "paperclip" structure with a tight turn as shown in Fig. 1 [10, 11]. Such triplex formation has been identified and confirmed by circular dichroism (CD) spectra, ultraviolet (UV) thermal melting, and proton nuclear magnetic resonance (NMR) spectroscopy [10, 11]. However, due to limited resolution, oligomers longer than 30 nucleotides or when the pH is higher than 7, the conformational characteristics are not readily resolvable by NMR. We found it pertinent to develop a more appropriate approach for revealing the DNA triplex structure of longer chain length.

Atomic force microscopy (AFM) has been proven a powerful tool for imaging and analyzing nucleic acids [12–18]. When applied to single molecules, AFM can be used to reveal structures and conformational dynamics of various types of nuclei acids [19–22]. The distinctive topographies of tight-turn DNA triplexes (in slightly acidic condition) and their unwound duplex or single strands (in neutral or basic condition) are readily distinguishable by single molecule AFM imaging in solution.

Here, we use AFM to visualize the triplex formation of four TFO's (Table 1), in solution, with similar repeating bideoxynucleotidyl AG or GA units (complemented by CT or TC) under either slightly acidic (pH 6.0) or slightly basic (pH 7.5–8.0) conditions. The significance of choosing TFO $(GA)_9$ and $(AG)_9$ sequences lies in the fact that they are found in the phosphatidylinositol transfer protein membrane-associated genes (PITPNM 3) of the human chromosome 17p13 [23]. PITPNM3 belongs to a family of membrane-associated phosphatidylinositol transfer domain-containing proteins that share homology with the Drosophila retinal degeneration B (rdgB) protein [23]. It is likely, then, that the stable tight turns of the triplexes may very well exist and affect the functions of the genes.

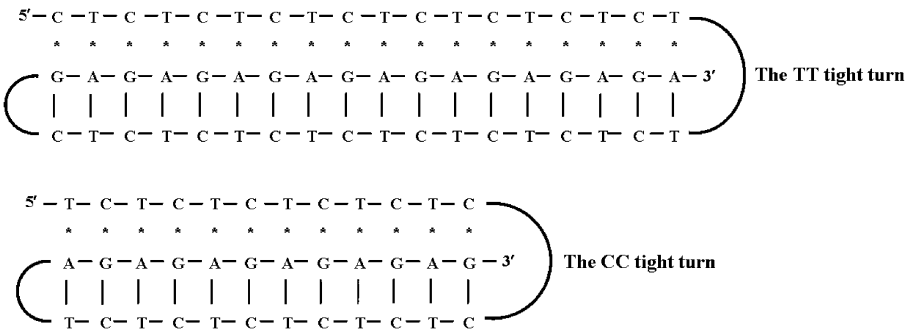

Fig. 1 A sketch of paperclip configuration of TFOs 5′-$(CT)_9(TC)_9(GA)_9$–3′ (CT9) and 5′-$(TC)_6(CT)_6(AG)_6$–3′ (TC6) triplexes with TT and CC tight turns, respectively. Vertical line indicates Watson Crick basepairing and asterisk indicates Hoogsteen base pairing

Table 1 A list of the oligodeoxyribonucleotides (TFOs) and their symbols.

Symbol	TFOs
CT9	5′-CTCTCTCTCTCTCTCTCT*TCTCTCTCTCTCTCTCTC***GAGAGAGAGAGAGAGAGA**-3′
TC9	5′-TCTCTCTCTCTCTCTCTC*CTCTCTCTCTCTCTCTCT***AGAGAGAGAGAGAGAGAG**-3′
CT6	5′-CTCTCTCTCTCT*TCTCTCTCTCTC***GAGAGAGAGAGA**-3′
TC6	5′-TCTCTCTCTCTC*CTCTCTCTCTCT***AGAGAGAGAGAG**-3′
CDC25	5′-TTCTTCTGATTCTCTCCTTT**GGAGAGAATCAGAAGAA**-3′

The Watson, Crick, and Hoogsteen motifs in the triplex are annotated by *bold face*, *italicized*, and *plain letters*. The underlined TTT moiety represents the loop linker of Watson and Click strands in CDC25, used a control duplex

In this report, we use AFM to explore the structural characteristics of DNA triplexes and duplexes formed from the 36-mer (i.e., CT6 and TC6 in Table 1) and 54-mer (CT9 and TC9) TFOs in buffer solutions. AFM is used, for the first time, to make direct measurements of a few new DNA triplexes that are composed of 12 to 18 nucleotidyl triad units containing either TT or CC tight turns. In addition, a duplex and a dangling single-strand DNA unwound from the triplex by dissociation of the Hoogsteen hydrogen bonds can also be identified on AFM images at pH 7.5 and 8.0. The results are consistent with CD observations for ensembles. One can use AFM in the direct observation of the DNA triplex to duplex or single-strand structural conversion.

Materials and Methods

Materials

All oligodeoxyribonucleotides (CT6, TC6, CT9, TC9, and CDC25), listed in Table 1, were purchased commercially (MDBio Inc. Taipei, Taiwan) with polyacrylamide gel electrophoresis purification and were used directly without further purification.

3-Aminoprophytriethoxy-silane (APTES), nickel chloride ($NiCl_2$), and other chemicals were obtained from Sigma (St. Louis, MO, USA). Mica is supplied locally.

Sample Preparation for AFM Imaging

The concentrations of all oligodeoxyribonucleotides were determined by the UV molar extinction coefficients at 260 nm, based on Fasman method [24]. Buffer solutions contain inorganic salts (100 mM NaCl and 20 mM $MgCl_2$) with 20 mM phosphates in pH 6.0 as triplex formation buffer and pH 7.5–8.0 as dissociation buffer; 1 μM of DNA triplex (at pH 6.0) and duplex (at pH 7.5–8.0) were made as stock solution [10, 11]. The AFM images of DNA were observed for concentrations ranging from 0.1 to 0.5 μM, diluted from the stock solution by either pH 6.0 or 8.0 buffer media.

Pretreatment of Mica with $NiCl_2$ and APTES

To immobilize DNA molecules for AFM imaging in solution, the supporting mica has to be pretreated by $NiCl_2$ or APTES; 20 μl of 10 mM $NiCl_2$ solution was placed on the surface of a freshly cleaved mica plate for 10 min. The mica surface was then rinsed with deionized water and dried with nitrogen gas. The mica was functionalized by APTES using the protocol

described earlier [25]. Fifteen microliters of 0.1% (*v*/*v*) APTES water solution was dropped on a freshly cleaved mica surface incubated for 10 min. Then, the surface was washed with deionized water and dried by nitrogen gas.

AFM Imaging

Sixteen microliters DNA solution, concentration ranging from 0.1 to 0.5 μM for different trials, was dropped on a $NiCl_2$ or APTES-pretreated mica surface for 10 min and then placed in a liquid cell (a small-sized Petri dish) filled with buffer. Images were taken by NanoWizard BioAFM (JPK Instruments, Berlin, Germany) in intermittent contact (tapping) mode in fluid. Silicon nitride cantilevers (Olympus) were used for scanning in liquid (BioLever, lever A). The spring constant of AFM cantilevers was 0.03 N/m, their resonance frequency was 10–40 kHz and tip radius 30 nm. All images (256×256 pixels) were scanned at a rate of 1 line/s up to 50 captured AFM images were collected and analyzed to determine the shapes and heights of DNA triplexes and duplexes. All the images presented were processed by a Line Fit Program for baseline subtraction and low-pass filtering. Further data analysis and graphics were performed by using a software SPM Imaging Processing v.3.0 (JPK Instruments, Berlin, Germany). Heights of DNA molecules were measured manually by using the "cross-section analysis" function of the same program.

CD Spectroscopy

CD spectra were obtained on a Jasco-815 CD spectropolarimeter (Jasco, Tokyo, Japan). The temperature was controlled at 25 °C by a Peltier PTC-423S/L unit. Dry nitrogen gas was blown through the cell compartment to expel oxygen and to prevent moisture condensation. A quartz cuvette with 1 cm path lengths was used.

In addition to four TFOs, a 17-nucleotidyl oligodeoxynucleotide (5′-TTCTT CTGATTCTCTCC; Table 1) from the gene of CDC 25 of Pneumernia carinii [27] was chosen for the CD spectrum of DNA duplex. By using the above sequence in our experiments, a hairpin duplex was designed by a corresponding complementary strand (5′-GGAGAGAAT CAGAAGAA) connected by TTT moiety (Table 1). This DNA oligonucleotide, designated as CDC25 (Table 1) can form a 17-base pair intramolecular by using TTT as a loop linker (26). This control can be used to demonstrate the structure of the non-triplex DNA in pH 7.0 using AFM in comparison with the dissociated state of triplex DNA in pH 8.0.

Results and Discussion

Direct Visualization of DNA Triplexes and Duplexes in Solution by AFM

Most of the AFM studies on DNA triplexes were focused on the ones with rather long sequences (thousands of base pairs) with exposure to the air [13, 19, 20]. Only a few were observed in solution [20, 26]. Here, for the first time, we used AFM to observe directly the shortest possible triplexes (~4 nm length, 12 nucleotidyl base triad units), containing a TT or a CC tight turn, in solution. Figure 2 presents typical solution images of DNA triplexes and duplexes. The triplexes appear generally in oval shape (Figs. 2a–c). The uniform lumps therein resemble curled-up structure of a triplex outlined on the left, according to Hansma et al. [13] and Chang et al. [26]. This implies that the TT and CC tight turns were formed [8]. On the other hand, all the images of the duplexes (Fig. 2d–g) show a diffuse "tail," which

may be interpreted as an unstructured single strand. A possible conformation is sketched on the left. This pH dependent DNA conformational change from triplex to duplex or single strand was never observed in other ensemble studies.

In fact, the observed widths of DNAs are larger than their true widths because of the finite width of our BioLever tips (see "Materials and Methods"). However, measurements of height are not affected by the tip radius. Their standard deviations are ≤0.1 nm for a flat mica surface. The key advantage of AFM is that the data collected can be displayed as an accurate 3D view of the sample, with sub-Angstrom accuracy in the Z (height) dimension. In our case, the height measurements of DNA triplexes and duplexes in AFM images provide valuable information. In Fig. 3, the histograms of heights are constructed from images of DNA under hydrated conditions without any drying artifacts. Twenty molecules images were analyzed for each histogram. Smaller oligomers do not bind strong enough to mica and, thus, are prone to detachment when rescanned [22]. In order to immobilize DNA molecules on mica for AFM scanning, the mica was pretreated by $NiCl_2$ or APTES (see "Materials and Methods"). Although the APTES-pretreated mica showed better performance with respect to the immobilization of DNA molecules, the surface, however, appeared more rugged relative to the small samples (12 and 18 triads DNA triplex and/or duplex). Thus, we selected only the DNA images obtained with untreated mica surface or on $NiCl_2$ pretreated mica for further analysis (Figs. 2, 3).

The population of heights for the DNA triplexes is prominent at 2.5 nm as shown in the histogram, a 3D topography of CT6 (at pH 6) and one cross-sectional trace in Fig. 3a and b.

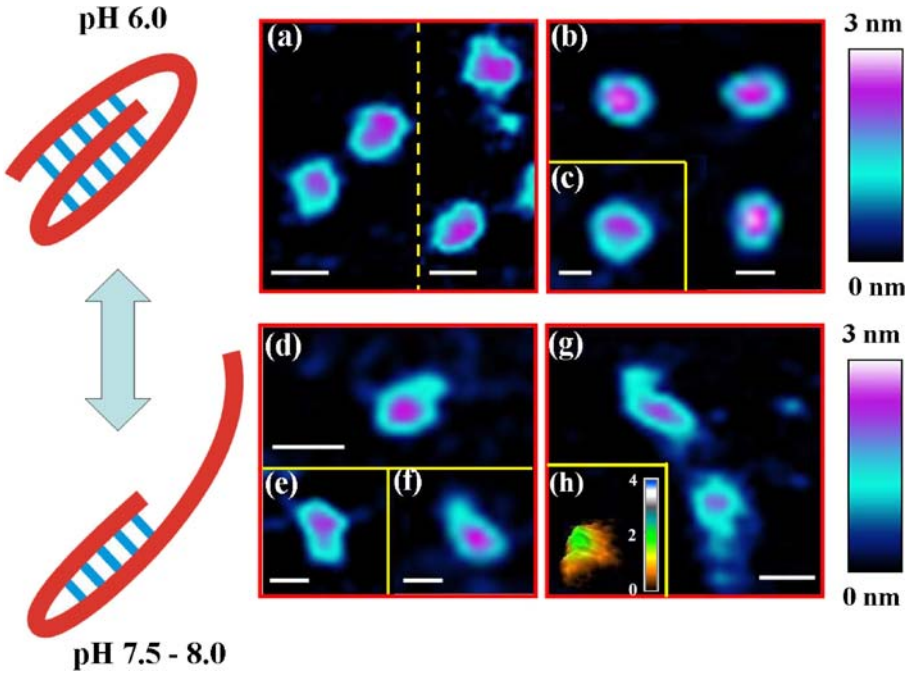

Fig. 2 AFM images showing the pH dependence in formation of TFO triplexes and duplexes. **a** CT6 at pH 6.0, **b** TC6 at pH 6.0, **c** CT9 at pH 6.0, **d** CT9 at pH 8.0, **e** TC6 at pH 8.0, **f** TC9 at pH 8.0, **g** TC6 at pH 7.5, **h** 3D image of the control sequence CDC25 of DNA duplex at pH 7. A *cartoon in the left-hand side* denotes a sketch of DNA triplex and duplex or single-strand structure. The *scale bars* represent 20 nm on all images

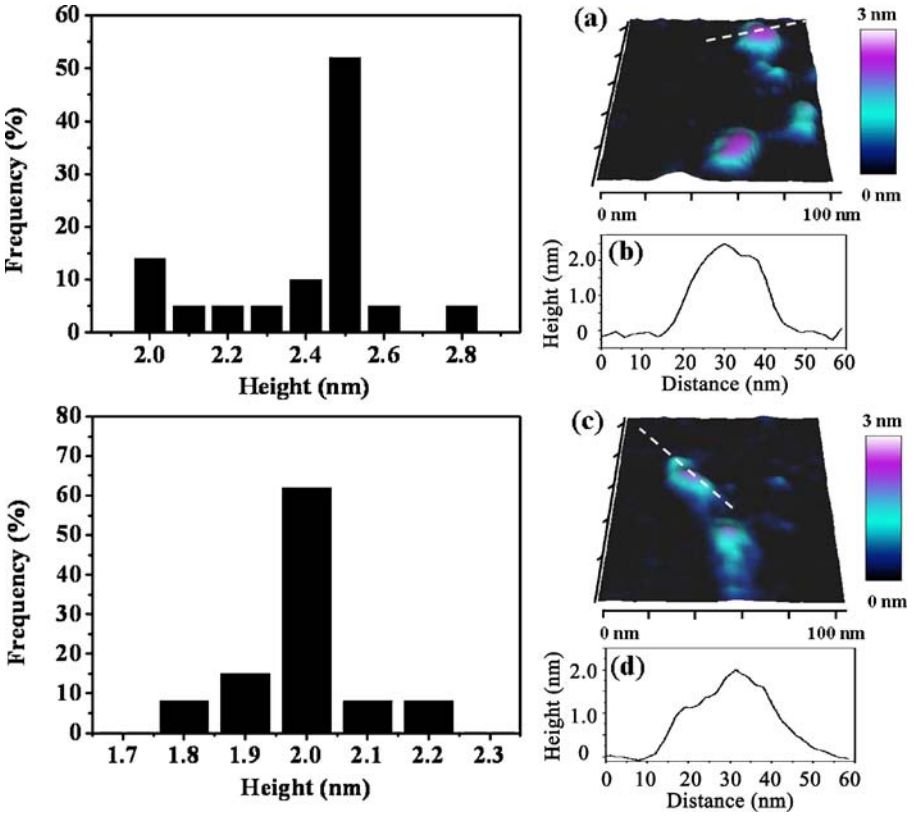

Fig. 3 *Right panel*: The 3D images of a representative triplexes (CT6 at pH 6.0, **a**) duplex (TC6 at pH 7.5, **c**); The profiles of the *dotted line* in (**a**) and in (**c**), respectively, show that the height of the triplex is 2.5 nm (**b**) and 2.0 nm for duplex with a shoulder (approximately 1.3 nm) for single-strand structure (**d**). *Left panel*: Histograms of the frequencies of triplex (*upper*) and duplex or single-strand (*lower*) structures. The total numbers of the measurement for triplex in *left panel* are 20 molecules and for duplex are 14 molecules

The average height of DNA triplexes (2.4±0.2 nm) is close to the height of the DNA triplex formed from a hairpin duplex and a single-stranded oligomer [26]. The population of heights for the DNA duplexes is dominant at 2.0 nm, as illustrated in the histogram, a 3D topography of TC6 (at pH 7.5) and one cross-sectional trace in Fig. 3c and d. The average height of DNA duplexes (2.0±0.1 nm) is consistent with the well-accepted theoretical value (2 nm) and the control DNA duplex of Fig. 2h for the heights of the DNA duplex in solution [15]. The height difference between the triplex and duplex DNA is clearly indicated here by AFM and is consistent with previous studies of triplexes by Tiner Sr. et al. [19] and Chang et al. [26]. The single-stranded tail can be seen in Fig. 3c, and its height is measured as 1.3 nm in Fig. 3d, respectively.

Paper-Clip Type Triplex and Duplex or Single-Strand Structure of CT6, TC6, CT9, and TC9 and the Duplex CDC25 by CD Spectra

CD spectra obtained on the four oligomers TC6, CT6, TC9, and CT9 at pH 6.0 (condition favors triplex formation) and 7.5–8.0 (condition favors duplex formation) are shown in Fig. 4A–D, respectively. All CD curves at pH 6.0 (dotted lines) show a trough at 210 nm

characteristic of paperclip triplex formation with repeated AG/CT/TC sequences [10]. The close similarity of CD spectra of all four oligomers at same pH to that of a known paperclip triplex, namely, 5′-TCTCTCCTCTCTAGAGAG, indicates that the G base at the 3′ end on each of the oligomers forms a CC/G base triad in the resulting triplex, as shown in Fig. 1. At a higher pH, the trough at 210 nm (heavy solid lines in Fig. 4) disappeared. Instead, a shallow trough at 240 nm (a typical of B-DNA character [28]) was observed for the same four oligomers. These results demonstrate that TC6, CT6, TC9, and CT9 change their triplex structure to B-DNA duplex form when the pH goes from slightly acidic (pH 6.0) to mild alkali (pH 7.5–8.0). This is consistent with the CD profile of control DNA duplex CDC25 in Fig. 4A (light gray line). It implies that a unimolecular complex is formed, which is consistent with the behavior of a paperclip type triplex model [8, 11]. Additionally, the conformational change of triplex and duplex or single-strand DNA is pH dependent and reversible as shown in the sketch of Fig. 2.

In general, the temperature is an important issue in physiological enzyme reaction. However, according to our previously experiences we find that the triplex structure is much sensitive to pH than temperature. Meanwhile, according to Gibbs free energy, we can find that the energy change of Gibbs free energy (ΔG) from pH 6.0 to 8.0 at 25 °C is around 2.73 Kcal/mol. However, for the $\Delta G'$ at 37 °C is around 2.84 Kcal/mol. Therefore, the energy difference between different temperatures $\Delta\Delta G$ is only 0.11 Kcal/mol. This energy change is smaller than single hydrogen bond (around 0.6 Kcal/mol) and this shall not affect the conformational change of DNA triplex. This is consistent to our previously studies [10, 11]. Therefore, we believe that the pH dependent effect shall be similar in physiological temperature.

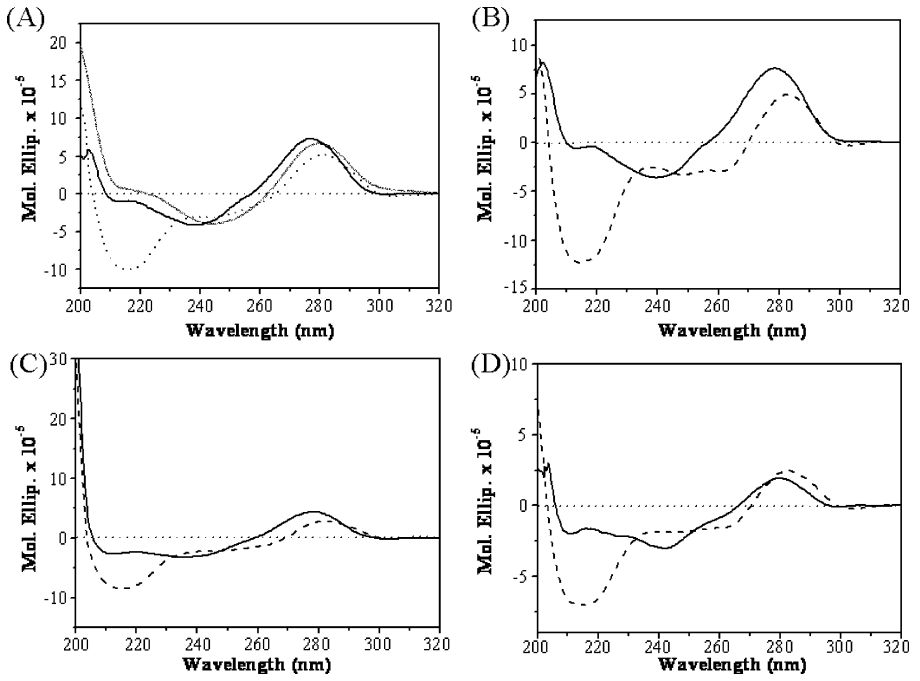

Fig. 4 CD spectra of: **A** TC6 at pH 6.0 (*dotted line*), 8.0 (*thick solid line*), and CDC25 at pH 7.0 (*thin gray line*); **B** CT6 at pH 6.0 (*dotted line*) and 8.0 (*thick solid line*); **C** TC9 at pH 6.0 (*dotted line*) and 8.0 (*thick solid line*); **D** CT9 at pH 6.0 (*dotted line*) and 8.0 (*thick solid line*)

Similar Sequences may Regulate Gene Expression in Biological Systems

The pH ranges of nucleus are from 7.55 to 7.80 of regular mammalian cell [29]. Meanwhile, the nucleoplasmic pH change may not drop under 7.1 [30]. Under this mild alkali pH environment, it is not easy to observe the DNA triplex formation. Therefore, the shape change of DNA triplex may not observe during the regular genome activity. However, the gene, PITPNM3, with extra T and/or C nucleotides at the loop regions between Crick/Watson and/or Watson/Hoogsteen segments which help stabilize the triplex formed in neutral pH environment [8, 10]. Therefore, according to the thermodynamics of Boltzmann distribution, a transient triplex structure of the gene may be observed during the genome activities, and the gene expression may be suppressed and modulated at such moment.

Meanwhile, by searching the BLAST of NCBI of human genome [31], we found that there are similar sequences of repeated dideoxynucleotidyl AG/CT/TC units in most human chromosomes. TFO $(GA)_9$ and $(AG)_9$ sequences are found in the phosphatidylinositol transfer protein membrane-associated genes (PITPNM 3) of the human chromosome 17p13, and are homologous to the Drosophila retinal degeneration B (rdgB) protein [23]. However, there are extra T and/or C nucleotides at the loop regions between Crick/Watson and/or Watson/Hoogsteen segments which help stabilize the triplex formed in neutral pH environment and this is consistent with Walter et al.'s study [9]. We believe that these sequences can form more stable DNA triplex structure in vivo and, thus, may play important roles in the control of gene expression and modulation.

Conclusion

We presented a practical and useful application of AFM to observe short DNA triplexes in solution. We chose some sequences of DNAs that exist in biological systems as paradigms. The shortest triplex observed is 4 nm (12 nucleotidyl units) long. Single strand, duplex, and triplex can be readily differentiated by the heights estimated from the AFM images. The results clearly indicate that molecular visualization of structures in DNA, as well as other biopolymers, can be done with AFM at the single molecular level which is not possible by other physical methods based on ensemble average observations.

Acknowledgements The authors thank for the BioAFM supported by Department of Biological Sciences and Technology at National Chiao Tung University, and National Nano Device Laboratories. The work is supported by National Science Council of Taiwan (NSC 95-2113-M-001-043-MY2 and NSC 97-2112-M-009-MY3 to LSK and CCC, respectively) and Academia Sinica.

References

1. Felsenfeld, G., Davies, D. R., & Rich, A. (1957). *Journal of the American Chemical Society*, *79*, 2023–2024. doi:10.1021/ja01565a074.
2. Wells, R. D., Collier, D. A., Hanvey, J. C., Shimizu, M., & Wohlrab, F. (1988). *The FASEB Journal*, *2*, 2939–2949.
3. Moser, H. E., & Dervan, P. B. (1987). *Science*, *238*, 645–650. doi:10.1126/science.3118463.
4. Franqois, J.-C., Saison-Behmoaras, T., Barbier, C., Chassignol, M., Thuong, N. T., & Helene, C. (1989). *Proceedings of the National Academy of Sciences of the United States of America*, *86*, 9702–9706. doi:10.1073/pnas.86.24.9702.
5. Sklenar, V., & Feigon, J. (1990). *Nature*, *345*, 836–838. doi:10.1038/345836a0.
6. Frank-Kamenetskii, M. D., & Mirkin, S. M. (1995). *Annual Review of Biochemistry*, *64*, 65–95.

7. Callahan, D. E., Trapane, T. L., Miller, P. S., Ts'o, P. O. P., & Kan, L. S. (1991). *Biochemistry*, *30*, 1650–1655. doi:10.1021/bi00220a030.
8. Kan, L. S., Pasternack, L., Wei, M. T., Tseng, Y. Y., & Huang, D. H. (2006). *Biophysical Journal*, *91*, 2552–2563. doi:10.1529/biophysj.106.084137.
9. Walter, A., Schütz, H., Simon, H., & Birch-Hirschfeld, E. (2001). *Journal of Molecular Recognition*, *14*, 122–139. doi:10.1002/jmr.528.
10. Chin, T. M., Lin, S. B., Lee, S. Y., Chang, M. L., Cheng, A. Y. Y., Chang, F. C., et al. (2000). *Biochemistry*, *39*, 12457–12464. doi:10.1021/bi0004201.
11. Pasternack, L., Lin, S. B., Chin, T. M., Lin, W. C., Huang, D. H., & Kan, L. S. (2002). *Biophysical Journal*, *82*, 3170–3180.
12. Ocaka, L., Spalluto, C. C., Wilson, I., Hunt, D. M., & Halford, S. (2005). *Cytogenetic and Genome Research*, *108*, 293–302. doi:10.1159/000081519.
13. Hansma, H. G., Sinsheimer, R. L., Li, M.-Q., & Hansma, P. K. (1992). *Nucleic Acids Research*, *20*, 3585–3590. doi:10.1093/nar/20.14.3585.
14. Hansma, H. G., Revenko, I., Kim, K., & Laney, D. E. (1996). *Nucleic Acids Research*, *24*, 713–720. doi:10.1093/nar/24.4.713.
15. Dahlgren, P. R., & Lyubchenko, Y. L. (2002). *Biochemistry*, *41*, 11372–11378. doi:10.1021/bi026102e.
16. Moreno-Herrero, F., Colchero, J., & Baró, A. M. (2003). *Ultramicroscopy*, *96*, 167–174. doi:10.1016/S0304-3991(03)00004-4.
17. Hansma, H. G. (2001). *Annual Review of Physical Chemistry*, *52*, 71–92. doi:10.1146/annurev.physchem.52.1.71.
18. Admcik, J., Klinov, D. V., Witz, G., Sekatskii, S. K., & Dietler, G. (2006). *FEBS Letters*, *580*, 5671–5675. doi:10.1016/j.febslet.2006.09.017.
19. Jiang, Y., Ke, C., Mieczkowski, P. A., & Marszalek, P. E. (2007). *Biophysical Journal*, *93*, 1758–1767. doi:10.1529/biophysj.107.108209.
20. Tiner Sr, W. J., Potaman, V. N., Sinden, R. R., & Lyubchenko, Y. L. (2001). *Journal of Molecular Biology*, *314*, 353–357. doi:10.1006/jmbi.2001.5174.
21. Klinov, D., Dwir, B., Kapon, E., Borovok, N., Molotsky, T., & Kotlyar, A. (2007). *Nanotechnology*, *18*, 225102–225109. doi:10.1088/0957-4484/18/22/225102.
22. Marsh, T. C., Vesenka, J., & Henderson, E. (1995). *Nucleic Acids Research*, *23*, 696–700. doi:10.1093/nar/23.4.696.
23. Shlyakhtenko, L. S., Potaman, V. N., Sinden, R. R., Gall, A. A., & Lyubchenko, Y. L. (2000). *Nucleic Acids Research*, *28*, 3472–3477. doi:10.1093/nar/28.18.3472.
24. Fasman, G. D. (1975). *CRC Handbook of Biochemstry and Molecular Biology* (vol. 1, 3rd ed.). Cleveland: CRC.
25. Lyubchenko, Y. L., Shlyakhtenko, L., Harrington, R., & Oden, P. (1993). *Proceedings of the National Academy of Sciences of the United States of America*, *90*, 2137–2140. doi:10.1073/pnas.90.6.2137.
26. Chang, C. C., Lin, P. Y., Chen, Y. F., Chang, C. S., & Kan, L. S. (2007). *Applied Physics Letters*, *91*, article *No.* 203901. doi:10.1063/1.2809406.
27. Gustafson, M. P., Thomas Jr, C. F., Rusnak, F., Limper, A. H., & Leof, E. B. (2001). *The Journal of Biological Chemistry*, *276*, 835–843. doi:10.1074/jbc.M007814200.
28. Gray, D. M., Hamilton, F. D., & Vaughn, M. R. (1978). *Biopolymers*, *17*, 85–106. doi:10.1002/bip.1978.360170107.
29. Seksek, O., & Bolard, J. (1996). *Journal of Cell Science*, *109*, 257–262.
30. Altan, N., Chen, Y., Schindler, M., & Simon, S. M. (1998). *The Journal of Experimental Medicine*, *187*, 1583–1598. doi:10.1084/jem.187.10.1583.
31. Levy, S., Sutton, G., Ng, P. C., Feuk, L., Halpern, A. L., Walenz, B. P., et al. (2007). *PLoS Biology*, *5*, 2113–2144. doi:10.1371/journal.pbio.0050254.